Modeling the environmental controls on tree water use at different temporal scales

Hailong Wang*, Huade Guan and Craig T. Simmons

School of the Environment, Flinders University, Adelaide, SA 5042, Australia

National Centre for Groundwater Research and Training, Flinders University, Adelaide, SA 5042, Australia

***Corresponding to** Hailong Wang (hailong.wang@abdn.ac.uk) +44 1224 272342

Present address: Northern Rivers Institute, School of Geosciences, University of Aberdeen, Aberdeen, United Kingdom, AB24 3UF

Emails of co-authors:

Huade Guan: huade.guan@flinders.edu.au

Craig T. Simmons: craig.simmons@flinders.edu.au

Abstract: Tree water use (E_c) can be simulated from environmental variables. Such E_c models can be categorized as firstly the Penman-Monteith (PM) equation where canopy conductance (g_c) is simulated from the Jarvis-Stewart (JS) approach, secondly the models modified from the JS approach that link E_c directly with environmental variables (MJS), avoiding the calculation of g_c, and thirdly process-based models that incorporate plant physiological functions. Tree water use and canopy conductance are constrained by the root-zone soil water supply and atmospheric demand (e.g., radiation, temperature, humidity and wind speed). This study aims to determine which type of E_c models performs better at the daily and hourly scales, and which influencing factors are more critical for E_c modeling at each time scale. We also examined the transferability of parameter values across temporal scales as this is a common issue that modelers need to deal with. The results show that the MJS and a simplified process-based model (BTA) models gave generally better simulations than the PM models at the hourly scale, and the best PM model gave comparable results to the best MJS model at the daily scale. BTA failed at the daily scale on the tree under water stress likely due to its incorporation of soil water availability into an integrated parameter. Soil water content function is more important for daily E_c modeling than hourly in all models. For MJS models, soil water content function has a stronger influence than air temperature on hourly E_c modeling, while no significant difference was observed in the PM models. Parameter values were not transferrable across temporal scales; and calibrating parameters in each season rather than in the first a number of days of all seasons helped improve the total E_c simulations.

Keywords: transpiration; sap flow; canopy conductance; soil moisture; stem water potential

1. Introduction

Vegetation covers 70% of the global land surface (Dolman et al., 2014), playing an important role in land surface hydrological and climatological processes, and coordinating land-atmosphere interactions in a wide range of spatial and temporal scales (Chen et al., 1996; Dickinson, 1987; LeMone et al., 2007). Vegetation affects water, carbon and energy transfer in the soil-plant-atmosphere system by altering surface albedo, roughness and soil macroporosity, intercepting rainfall and transpiring water from soil layers (Ivanov et al., 2008). Several studies confirmed that vegetation transpiration (E_c) contributes a large proportion of total global terrestrial evapotranspiration (ET) (Jasechko et al., 2013; Miralles et al., 2011; Schlaepfer et al., 2014; Schlesinger and Jasechko, 2014; Wang et al., 2010). Although the reported numbers vary over different ecosystems, they highlight the importance of quantifying rates of vegetation water use to understanding of land-atmosphere interactions.

Transpiration at the tree and plot scales can be estimated using sap flow techniques (Ford et al., 2007; Hatton et al., 1995). Alternatively, transpiration can be estimated from potential transpiration by applying stress functions related to different environmental variables, e.g., temperature, vapor pressure deficit, solar radiation, soil water content/potential and plant water potential (Damour et al., 2010; Jarvis, 1976; Tuzet et al., 2003; Wang et al., 2014), and CO_2 concentration (Ball et al., 1987). Such an approach can be applied over various spatial scales, and has long been incorporated into land surface and atmospheric models (Dai et al., 2004; Dickinson et al., 1991; Noilhan and Planton, 1989). The reduction of potential E_c is often realized by replacing the canopy conductance g_c under the optimal conditions in the Penman-Monteith (PM) equation with

the one considering the environmental stresses, well known as the Jarvis-Stewart (JS) approach (Jarvis, 1976; Stewart, 1988). In this study, PM equation with the embedded JS-g_c model was labeled as the PMJS method.

Apart from studies using the Penman-Monteith equation, there have been several attempts to estimate E_c directly from environmental variables. For example, Whitley et al. (2009; 2013) applied such method for transpiration simulations at different Australian forest sites. Garcia et al. (2013) also applied a similar E_c model in a woody savannah in Mali and grassland in Spain using in-situ and satellite data. These models estimate transpiration from a maximum rate by applying a set of functions of the relevant environmental variables, based on a similar assumption with the JS-g_c approach that the stress from environmental variables on plant water use is independent of each other. Essentially, these models are modified from and considered as variants of the JS approach. Compared to the PMJS method, they are much simpler to fit, require fewer measurements and specifically avoid the circularity of inverting the PM equation to calculate g_c from E_c and then using the PM again to estimate E_c from g_c. To differentiate this way of E_c modeling from the PMJS, we labeled this type of model as MJS in this study.

In addition, there have also been g_c/E_c models based on understanding of the physical processes at cellular level, i.e. exploration on plant guard cell functions and the hydro-mechanical and biochemical influences in and around guard cells (Buckley and Mott, 2002; Dewar, 2002; Franks et al., 1998; Gao et al., 2002). On the basis of a series of assertions, Buckley et al. (2003) developed a process-based g_c model with clear physiological interpretations and later simplified it (Buckley et al., 2012) for transpiration

as well as canopy conductance modelling. The simplified model (labeled as BTA model hereafter) has two to four parameters that are related to reduced processes and properties, allowing us to have a transparent understanding about how those parameters respond to environmental changes (Buckley et al., 2012).

Widely used environmental variables in E_c/g_c modelling can be divided into two groups as to how they affect tree water uptake, i.e. atmospheric demand and water supply. The demand group includes solar radiation, air temperature and humidity, and wind speed. Air temperature function is often neglected in g_c models that use humidity as one variable (Lhomme et al., 1998; Mascart et al., 1991). Vapor pressure deficit is also favorably used for E_c/g_c modeling, and is highly correlated with air temperature (Alves and Pereira, 2000). Some studies included both functions of air temperature and vapor pressure deficit while others used only one (Damour et al., 2010). The supply group mainly refers to the root-zone soil moisture, determined by water content, soil hydraulic properties and root distribution. It is worth mentioning that plants respond to soil water potential rather than soil water content (Gregory and Nortcliff, 2013; Marshall et al., 1996; Mullins, 2001; Verhoef and Egea, 2014). Soil water content in most studies was measured in shallow soil layers, up to 2 m deep and usually 0.5 m (Whitley et al., 2009). It is uncertain whether such measurements can capture the entire picture of root-zone water availability (Schulze et al., 1996), especially for deep rooted trees. It is the gradient of water potentials in soil, stem and leaves that drives water transport in the soil-plant system (Vandegehuchte et al., 2014). Plant water potential is a sensitive indicator for vegetation water status (Choné et al., 2001; Nortes et al., 2005) and can be in equilibrium in the whole soil-plant system at predawn unless significant nocturnal transpiration (Palmer et

al., 2010; Richter, 1997). Therefore, predawn plant water potential is a better approximate of root-zone soil water availability than the shallow layer soil water content. Previous studies have proved the feasibility of using predawn stem water potential to indicate plant water stress and simulate canopy conductance (Wang et al., 2014; Yang et al., 2013).

Despite the wealth of literature in considering the supply factor for E_c and g_c modeling, some studies showed success without including this factor (Bunce, 2000; Leuning, 1995; Whitley et al., 2013). Typical examples are transpiration from trees with groundwater access by deep roots (Eamus and Froend, 2006) and from trees growing in riparian sites (O'Grady et al., 2006). However, at other sites, it is difficult to determine the significance of soil water availability for E_c or g_c modeling without long-term monitoring of the relevant variables. Furthermore, soil water availability has seasonal variations in correspondence with precipitation (Findell and Eltahir, 1997), which means that the necessity to include a soil water stress function may vary seasonally. Note that seasonality of soil water content is also strongly influenced by plant water uptake.

Usually parameters need to be re-calibrated when models are applied at a different site or temporal scale, however, in many land surface models parameters are prescribed for lumped vegetation functional types, for example, evergreen needle-leaf trees, deciduous broad-leaf trees, etc. (Chen and Dudhia, 2001). These parameter values remain the same for simulations at various temporal/spatial scales in practice. This can be problematic given the nonlinear relationship between transpiration and the environmental variables, and the fact that environmental variables' values differ from one spatial-temporal scale to another.

This study examined the performance of selected PMJS, MJS and BTA E_c models at daily and hourly scales. By comparing the simulation results, we focus on the following four specific questions: (1) Which type of E_c modeling approach performs better? (2) Are soil water content and air temperature functions critical for E_c simulation? (3) At which time scale and in which season do soil water function and air temperature functions pose a stronger influence on E_c modeling? (4) Are parameter values transferable across different temporal scales (daily and hourly) for the same E_c model?

2. Methodology

2.1. Site and measurements

The study site is on the campus of Flinders University (138°34′28″E, 35°01′49″S), located in a Mediterranean climate zone. Annual mean temperature is about 17 °C, and annual rainfall is around 546 mm, most of which occurs in May to September (Guan et al., 2013). Ground surface is covered by sparse trees with short shrubs and grass at substrate. Soil type is characterized as sandy mixed with gravel. The soil condition makes it difficult to bury soil moisture probes in deep root-zone soil layers near the tree. Therefore, as discussed in previous work (Wang et al., 2014; Yang et al., 2013) stem water potential was used as an indicator of root-zone soil water availability. We conducted measurements on four Drooping Sheoak (*Allocasuarina verticillata*) trees over different time periods in 2011, 2012 and 2014. The discussion in this study is based on one tree with continuous measurements in January to April and October to December in 2012. Data from the other three trees covered shorter periods, and were mainly for consistency check on results of canopy conductance modelling among trees in a previous work (Wang et al., 2014), and not included in this study.

Sap flow was monitored at 30-min intervals in the tree trunks at 1.3 m above ground using the compensation heat-pulse technique (Green and Clothier, 1988). Three thermocouples were embedded inside each temperature probe at the depths of 5, 15 and 25 mm underneath the cambium. One temperature probe was installed 10 mm above the heater and the other 5 mm below the heater. Two sets of such probes were installed in the south and north sides of the tree. Transpiration was calculated from heat transport velocity and corrected for wounding, sapwood area, volume fraction of wood and water following Green et al. (2003).

Stem water potential (ψ_{st}) was measured at 15-minute intervals using a PSY1 Stem Psychrometer (*ICT International Pty Ltd., NSW, Australia*), which was developed by Dixon and Tyree (1984) and became commercially available in the recent years. PSY1 measures the temperature of sapwood surface and chamber air, and stem water potential is estimated from the water potential in the chamber corrected with the wood-air temperature gradient (Dixon and Tyree, 1984). Predawn stem water potential (ψ_{pd}) was taken as the average of ψ_{st} between 3:00 am and 5:00 am, when water potentials in the tree and root-zone soil have reached an equilibrium state after water redistribution in the plant-soil system.

A weather station was set up at a location nearby to measure the micrometeorological variables, including air temperature, solar radiation, rainfall, wind speed, and atmospheric pressure, etc. All measurements were aggregated to hourly and daily values for model runs and comparisons. Data on rainy days were excluded in this study for model parameterization and comparison.

2.2.Models briefing

2.2.1. PM equation with g_c simulated by the Jarvis-Stewart approach

The PM method is formulated in equation (1). Canopy conductance g_c is estimated from environmental variables following the Jarvis-Stewart (JS) pattern in equation (2).

$$E_c = \frac{\Delta A_c + \rho_a C_p D g_a}{\rho_w \lambda [\Delta + \gamma(1 + g_a / g_c)]} \quad (1)$$

$$g_c = g_{\max} LAI \cdot f(D) f(T) f(R_s) f(\psi) \quad (2)$$

In equations (1-2), g_a is the aerodynamic conductance [m/s]; γ is the psychrometric constant [kPa/^{o}C]; λ is the latent heat of vaporization [MJ/kg]; E_c is the tree water use calculated from sap flow measurements; Δ is the slope of saturation vapor pressure-temperature curve [kPa/^{o}C]; A_c is the available energy allocated to canopy [MJ/(m^{2}h)]; C_p is the specific heat of air at constant pressure [MJ/(kg^{o}C)]; D is the vapor pressure deficit in the air [kPa]; ρ_a and ρ_w are the density of air and water [kg/m^3]. g_{max} is the maximum stomatal conductance [m/s]. LAI is the leaf area index. ψ is the stem water potential [MPa]. Predawn stem water potential (ψ_{pd}) is used for daily E_c or g_c simulation.

Here we denote equations (1-2) as the PMJS4 model, as it considers the effects of four environmental variables. In order to test the significance of stress functions of air temperature and soil water content, we made modifications to the PMJS4 by neglecting *f(T)* and *f(ψ)*, respectively, and the relevant models are denoted as the PMJSψ and PMJST. Equations (3-6) are the selected stress functions for the four variables based on a previous study (Wang et al., 2014).

$$f(R_s) = \frac{R_s}{R_s + k_{Rs}} \cdot \frac{R_{sm} + k_{Rs}}{R_{sm}} \quad (3)$$

$$f(D) = e^{-k_D D} \quad (4)$$

$$f(T) = 1 - k_T (T_o - T)^2 \quad (5)$$

$$f(\psi) = \frac{1}{1 + (\psi / \psi_m)^{k_\psi}} \quad (6)$$

R_{sm} is the approximate maximum solar radiation, set as 1000 W/m^2 for hourly and 350 W/m^2 for daily simulations according to measurements. k_{Rs} [W/m^2], k_D [k/Pa], k_T [-], T_o [^{o}C], k_ψ [-] and ψ_m [MPa] are fitting parameters.

2.2.2. Modified Jarvis-Stewart approach

The models described in this section are modified from and considered as variants of the JS approach; they omit the canopy conductance calculation, but estimate tree water use directly from a set of environmental stress functions. These models have simpler structures and a smaller number of parameters compared to the PMJS models. Whitley et al. (2013) estimated tree water use directly from solar radiation, vapor pressure deficit and soil water content. Based on their model, here we supplemented a temperature function, replaced the soil water content function with a stem water potential function in equation (6), and discarded the parameter k_{D2} in their vapor pressure deficit function which is an addend to D in the denominator of equation (8), as this parameter is redundant for shaping the response curve. The final modified model is given in equation (7) and referred to as MJS4 for the same reason as PMJS4. In equations (7-8), E_{max} is the

maximum transpiration rate [mm/h or mm/d]. $f^{\wedge}(D)$ is the modified function of vapor pressure deficit. k_D is a fitting parameter. D_{peak} [kPa] is the value of D at which E_c is maximized. $f(R_s)$, $f(T)$ and $f(\psi)$ are the same with equations (3), (5) and (6). To facilitate the model comparison, further modifications were made to MJS4 by neglecting $f(T)$ and $f(\psi)$, respectively, referred to as MJSψ and MJST accordingly.

$$E_c = E_{\max} f^{\wedge}(D) f(T) f(R_s) f(\psi) \tag{7}$$

$$f^{\wedge}(D) = \exp\left\{-\frac{k_D (D - D_{peak})^2}{D}\right\} \tag{8}$$

2.2.3. A simplified process based model

Buckley et al. (2012) simplified a previously developed process model (Buckley et al., 2003) for transpiration estimates, given in equation (9), and denoted in this study as the BTA model.

$$E_c = \frac{E_{\max} D_s (R_s + R_{s0})}{k + bR_s + (R_s + R_{s0}) D_s} \tag{9}$$

k and b are integrated model parameters. E_{max} is the maximum transpiration rate which includes the effect of soil water availability. D_s is the leaf to air vapor pressure deficit, and can be approximated with the air vapor pressure deficit (D) when canopy is coupled aerodynamically. We use D in this study due to the lack of leaf temperature measurements. The parameter R_{s0} allows night-time transpiration for sub-daily simulation which is the particular strength over other models. In this study, however, Drooping Sheoak tree night-time sap flow is negligible (based on the 15-min stem water potential

data), and because the Jarvis-Stewart approach is incapable of capturing the nocturnal transpiration, we prescribed R_{s0} as zero for inter-comparison among models. The BTA model uses only solar radiation and vapor pressure deficit in the formulation, and has even fewer parameters than PMJS and MJS models.

It should be noted that the original g_c model in Buckley et al. (2003) includes more variables, such as leaf-specific hydraulic conductance, soil water potential, epidermal osmotic pressure, turgor pressures of epidermal and guard cells, and 'guard cell advantage' which incorporates the effects of light, CO_2 and hormonal signals from roots (ABA). In their later work (Buckley et al., 2012) some of the variables were lumped together as invariant parameters and tested to be well performed for sap flux simulations on a number of trees. Those parameters have clear physical meanings that are related to plant physiology under biochemical and hydro-mechanical influences. Although in a simple form, the simplified models should be differentiated from empirically developed ones.

Buckley et al. (2012) also provided a simplified conductance model as follows:

$$g_c = \frac{E_m(R_s + R_{s0})}{k + bR_s + (R_s + R_{s0})D_s} \quad (10)$$

where E_m, k and b are integrated model parameters. In this study, canopy conductance was also estimated from equation (10) and used in the PM approach for transpiration estimate to compare with other models. Hereinafter, PMB denotes PM equation with the g_c simulated from equation (10) for E_c calculation.

2.3.Parameter optimization and model comparison

For daily simulations, the data were divided into two groups (one contains data in the order of 1, 3, 5 … and the other 2, 4, 6… respectively). The first group was used to train the model, and the second group was used to test the model. For hourly simulations, we used 60-day hourly data to train the model and used another 60-day data to test the model. Furthermore, we grouped the data in spring (September, October and November), summer (December, January and February) and autumn (March, April and May), and then trained the model using the first 20 days of data in each season, and tested the model using another independent 20 days of data. Note the data mentioned above and elsewhere in this study do not include the data on rainy days.

Parameters were obtained using the DiffeRential Evolution Adaptive Metropolis (DREAM) model (Vrugt et al., 2009), which runs multiple different chains simultaneously for global exploration and automatically tunes the scale and orientation of the proposal distribution in randomized subspaces during the search. DREAM was performed for each model by 20,000 iterations. We evaluated the model performance using the slope (k) and coefficient of determination (R^2) of linear regression between the measured and simulated E_c with a zero intercept, and the root mean square error ($RMSE$).

3. Results and discussion

3.1.Environmental conditions and tree water use

Part of the measurements is demonstrated in Figure 1 at hourly intervals. Data in rainy days are not shown. The transpiration and canopy conductance reached maximum values (3.0 mm/d and 0.015 m/s respectively) in early spring (October), when the rainy season

just ended, so there was sufficient water storage in the soil for trees to transpire. In the meantime, solar radiation was increasing, resulting in an optimal condition for transpiration and tree growth. In Figure 1, temperature has similar dynamics as vapor pressure deficit, which reflects a high interdependency between these two variables. Larger transpiration rates occur at higher (close to zero) stem water potential which reflects the effects of root-zone soil water supply on transpiration. In December when the site became hotter and drier, stem water potential decreased. Stem water potential data indicate that Drooping Sheoak recovered xylem water storage in night-time and had reached an equilibrium state before predawn. The average difference between the maximum and minimum stem water potential was around 1.0 MPa for clear days in dry season.

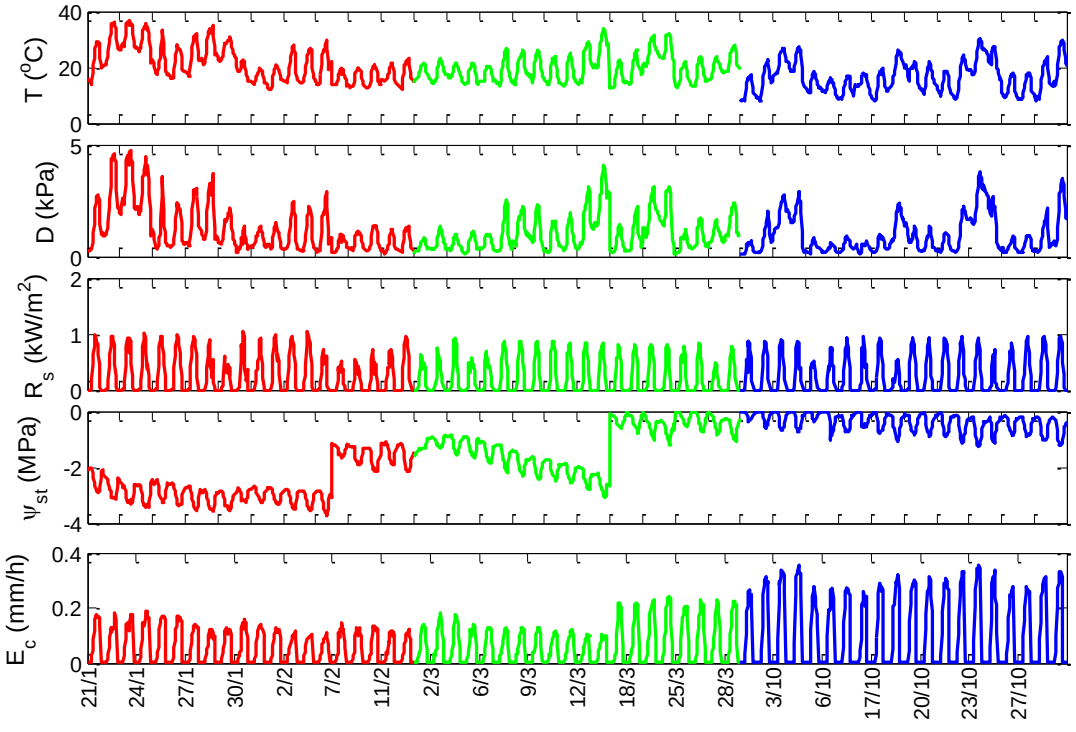

Figure 1 Demonstration of partial hourly environmental variables and tree water use (E_c)

in each season. Horizontal axis labels are the measurement dates in 2012. Red is for summer days, green is for autumn days and blue is for spring days

3.2.Model comparison

3.2.1. Hourly E_c modeling

We first evaluated the models at hourly scale by comparing the simulated and measured E_c for 60 days in Figure 2. All these models were able to present diurnal variation of E_c, however, PMJST, PMB, MJST and BTA overestimated E_c in summer and autumn days when it was hot and dry. These models are lack of explicit constraint from soil water function in their model construction, although the parameter E_{max} in the BTA model includes the effects of soil water availability, when integrated as a lumped parameter instead of the variables themselves the representation of soil water availability effects seems weakened. In the meantime, PMJS4 and PMJSψ underestimated E_c in summer. In spring days E_c was more underestimated by the MJS and BTA models than the PM models. The day-to-day difference of E_c given by MJST and BTA were relatively small (Figure 2*c-d***Error! Reference source not found.**), which indicates that these two models may fail to account for the effects of day-to-day variations of soil water availability.

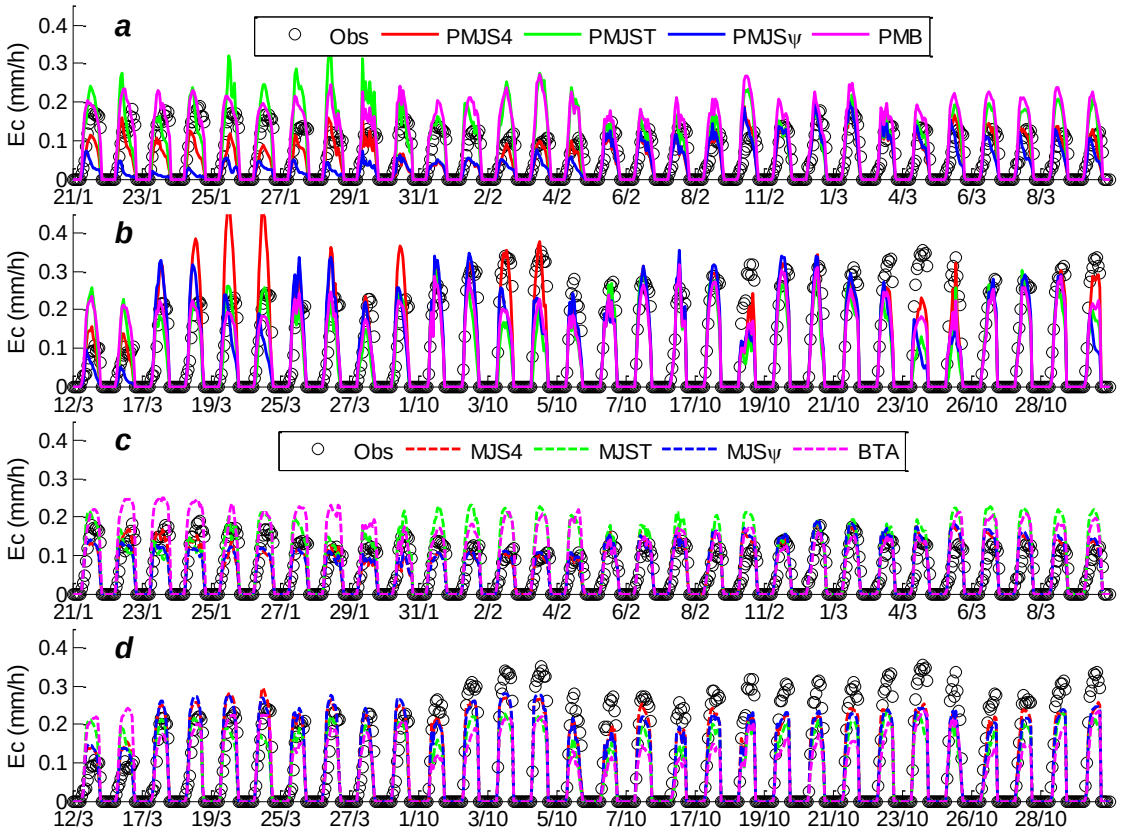

Figure 2 (*a*-*b*) Comparison of E_c simulated by PM models against observations at hourly scale; (*c*-*d*) comparison of E_c simulated by MJS and BTA models against observations at hourly scale. *Obs* is measured E_c.

The scatter plot of simulated and measured E_c, and the linear regression k (slope), R^2 and *RMSE* between them are given in Figure 3 and Figure 4, respectively. The MJS and BTA models give generally better fitting than the PM models, reflected by higher k, R^2 and lower *RMSE*. The PMJS4 and MJS4 outperformed other models in their own corresponding group, and MJS4 gives better fittings than PMJS4 (Figure 4). Note that the PMB gave a slightly higher fitting slope than the PMJS4, but both R^2 and *RMSE* are

lower from the PMB. In other words, models containing all four environmental variables perform better than those with reduced variables. Therefore, at hourly scale, *f(T)* and *f(ψ)* are both significant for transpiration modeling and should not be neglected in the E_c models.

Comparison among models with reduced environmental variables shows that the *k*, R^2 and *RMSE* all imply a better fitting by MJSψ than MJST. This indicates that the effect of soil water function was stronger than that of temperature function in the MJS models. On the contrary, no significant difference is observed between the PMJST and PMJSψ models.

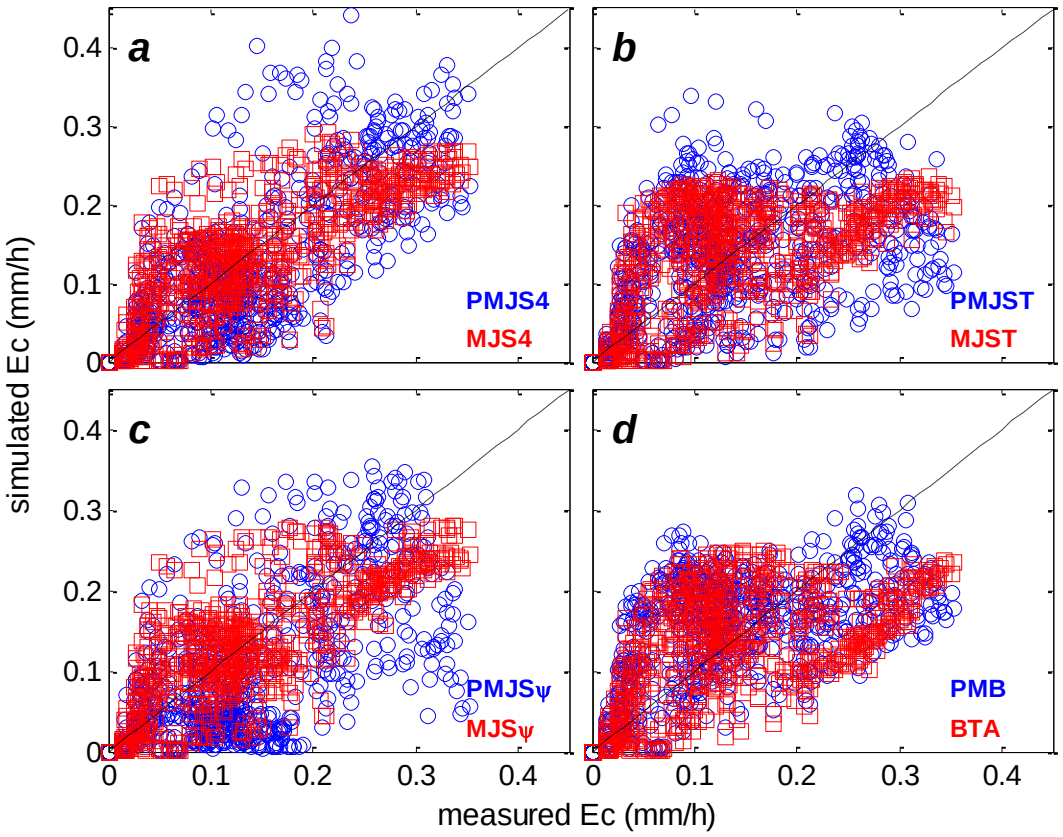

Figure 3 Comparison between hourly E_c from sap flow measurements and E_c simulated by PM, MJS, and BTA models. Dashed lines are 1:1 lines

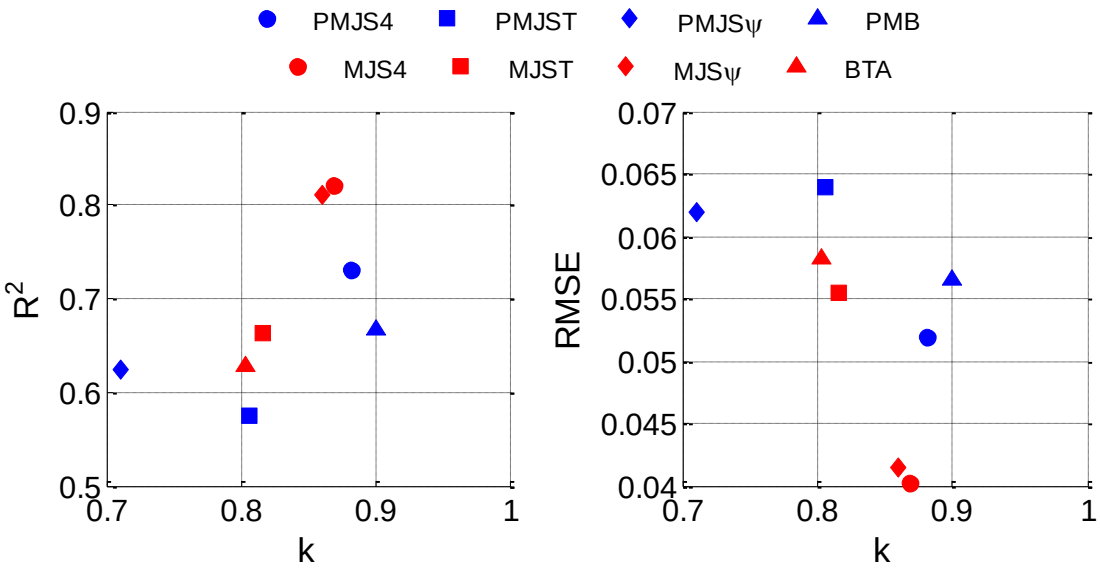

Figure 4 Statistical results of linear regression between measured hourly E_c and simulations by the PM, MJS and BTA models. k is regression slope, R^2 is coefficient of determination, and *RMSE* is root mean square error, in mm/h.

3.2.2. Hourly E_c modeling in individual seasons

E_c was simulated separately for spring, summer and autumn to examine the effects of $f(\psi)$ and $f(T)$ with distinct temperature and soil water condition differences. Results from the PM methods are given in Figure 5 and Figure 6. Statistical results of comparison between simulated and measured transpiration are shown in Table 1. Figure 5 shows a good fitting between the simulated and measured E_c in all seasons, although overestimation around midday for a few days in each season is observed. The best agreement between the simulated and measured E_c appears in spring by PMJS4 (Figure 6). Comparing the k, R^2

and *RMSE* given by PMJS4 and PMJST implies that inclusion of a $f(\psi)$ resulted in great improvement on E_c simulation in summer, but had little influence in spring and autumn. Similarly, comparison between PMJS4 and PMJSψ indicates that inclusion of a *f(T)* improved model performance in summer, but deteriorated model performance in spring and autumn. The negative impacts of a temperature function on tree water use modeling, which is not very strong in this study, have also been reported elsewhere (Sommer et al., 2002; Whitley et al., 2013; Wright et al., 1995). We also found in a previous work (Wang et al., 2014) that the temperature function, not used together with a humidity function but with a vapor pressure deficit function, caused a problem for physical interpretation of the environmental stress functions. This calls for attention to parameterizing site-specific E_c models from environmental variables. Model PMB reproduced diurnal variations of E_c with greater overestimation than other models especially in some autumn days (Figure 5*c*). This may be due to the model structure which expresses the effects of soil water stress through a lumped parameter E_m in equation (10), rather than a dynamic soil water availability function, although the parameter E_m in Buckley et al. (2012) includes the effect of soil water potential. The treatment of the relevant specific variables as a fixed parameter (E_m) seems not holding in our study, which is not certain whether it is related to species.

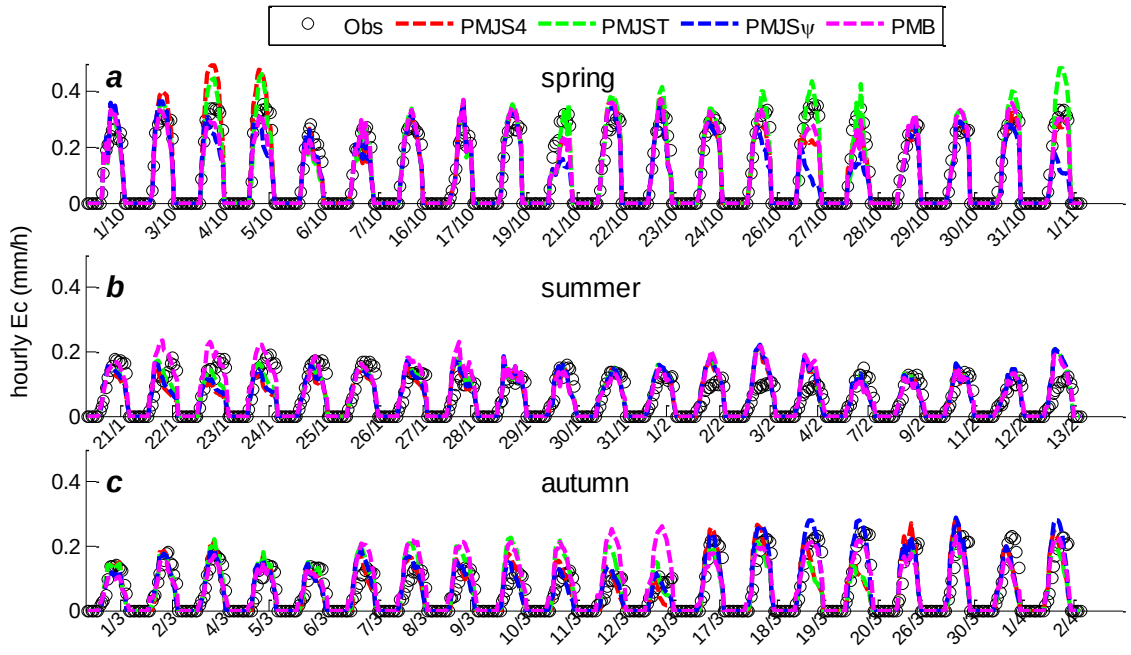

363

364 Figure 5 Hourly E_c simulated from the PM approach compared to sap flow measurements in (*a*)

365 spring; (*b*) summer and (*c*) autumn

366

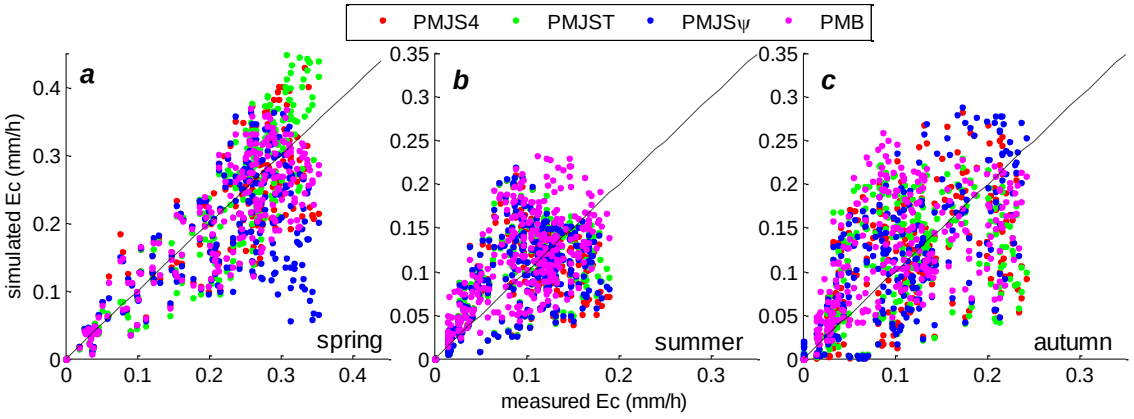

367

368 Figure 6 Scatter plots of hourly E_c simulated from the PM models compared to sap flow

369 measurements in (*a*) spring; (*b*) summer and (*c*) autumn. Dashed lines are 1:1 lines

Table 1 Statistical results of comparison between simulated and measured hourly transpiration by the PM approach in Figure 5 and Figure 6. *k* is linear regression slope, R^2 is the coefficient of determination, *RMSE* is root mean square error, in mm/h.

Models	Spring			Summer			Autumn		
	k	R^2	*RMSE*	*k*	R^2	*RMSE*	*k*	R^2	*RMSE*
PMJS4	0.98	0.89	0.0442	0.96	0.68	0.0367	0.87	0.59	0.0500
PMJST	1.06	0.93	0.0402	0.88	0.63	0.0384	0.88	0.63	0.0474
PMJSψ	0.80	0.79	0.0620	0.92	0.65	0.0380	0.89	0.73	0.0422
PMB	0.93	0.67	0.0377	1.08	0.75	0.0361	0.89	0.65	0.0484

Figure 7 and Figure 8 give the results from the MJS and BTA models, which gave overall better simulations than the PM models. The statistical results of comparison between simulated and measured hourly transpiration are given in Table 2. The best fitting between simulated and measured E_c was also in spring. The models including all four environmental variables did not show obvious superiority over the models without *f(T)* or *f(ψ)*. However, we observe that soil water function had a stronger influence on tree water use modeling in autumn than spring and summer (Figure 8*c*). Simulated E_c in Figure 7 underestimated the maximum sap flow measurements around midday for some days. Using data of other days to train and test the models did not eliminate the phenomenon. We checked the solar radiation data on those days, and found that the underestimation occurred on cloudy middays, when solar radiation did not reach the maximum value as on clear middays. This implies that the models are limited by solar radiation functions on cloudy days. BTA E_c model (equation 9) gave very similar simulations with the three MJS models, especially in spring, which is encouraging because it requires the minimum number of input variables and parameters compared to its counterparts. In autumn BTA E_c model gave the worst simulations compared to other models and in other seasons.

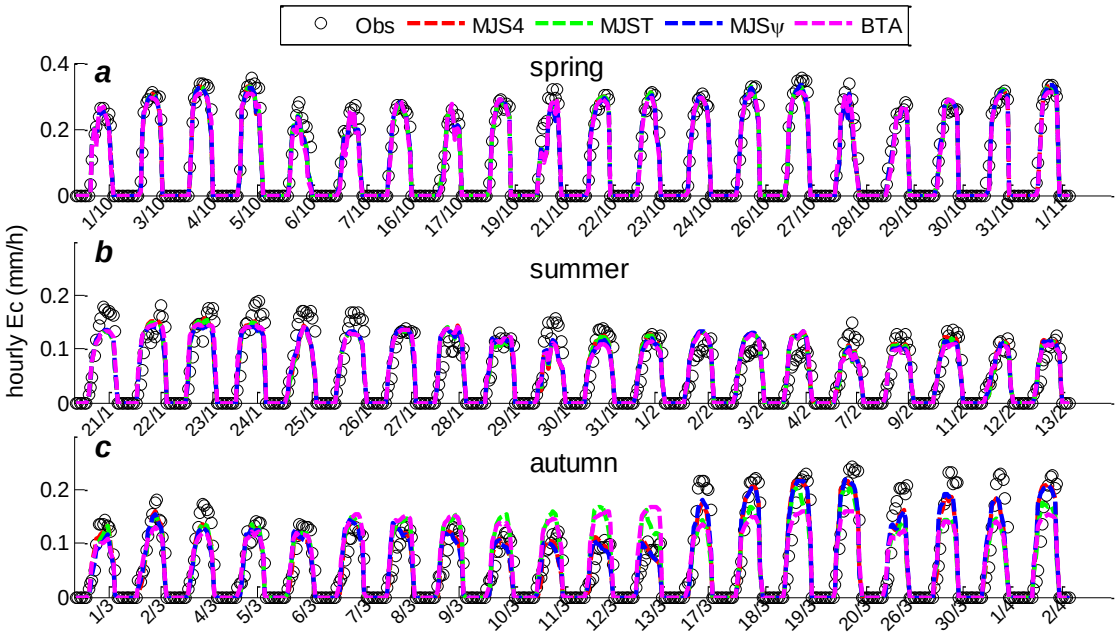

Figure 7 Tree water use simulated from the MJS, MJST, MJSψ and BTA models in comparison with sap flow measurements at an hourly scale for (*a*) spring, (*b*) summer and (*c*) autumn

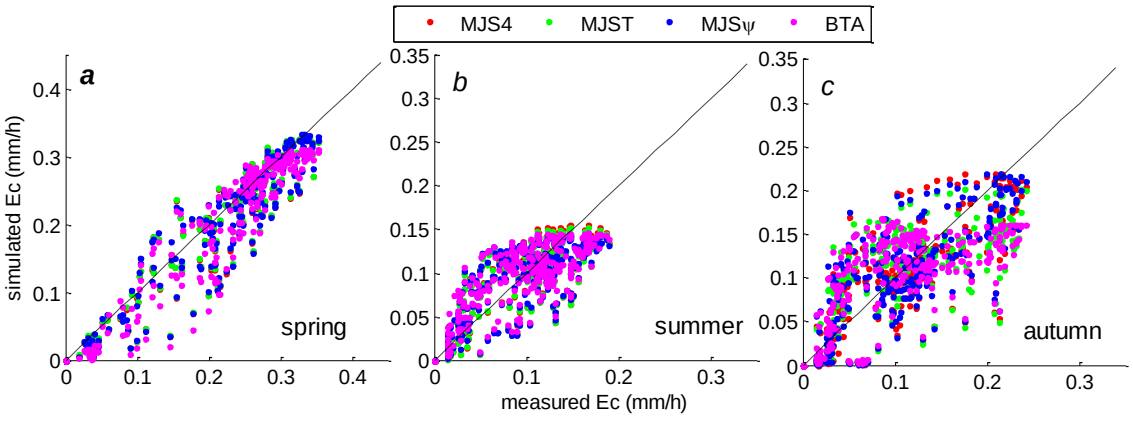

Figure 8 Scatter plots of hourly E_c simulated from the MJS and BTA models compared to sap flow measurements in (*a*) spring; (*b*) summer and (*c*) autumn. Dashed lines are 1:1 lines

Table 2 Statistical results of comparison between simulated and measured hourly transpiration by the MJS and BTA models in Figure 7 and Figure 8. *k* is linear regression slope, R^2 is the coefficient of determination, *RMSE* is root mean square error, in mm/h.

Models	Spring			Summer			Autumn		
	k	R^2	*RMSE*	*k*	R^2	*RMSE*	*k*	R^2	*RMSE*
MJS4	0.93	0.96	0.0250	0.92	0.83	0.0245	0.89	0.81	0.0316
MJST	0.94	0.96	0.0244	0.91	0.83	0.0244	0.86	0.74	0.0369
MJSψ	0.94	0.96	0.0247	0.91	0.83	0.0246	0.89	0.81	0.0321
BTA	0.93	0.96	0.0258	0.92	0.67	0.0239	0.83	0.67	0.0389

The study site is under optimal conditions (i.e. trees transpire at a rate close to the potential rate) for tree water uptake in spring, because most of the annual rainfall occurs in the previous season at this site (Guan et al., 2013), resulting in sufficient water storage in the root zone for trees to transpire, and the solar radiation input also increases in this season (Figure 1). The relationships between transpiration and the four environmental variables (Figure 9) show that the spring data form the upper envelopes of all the data points. The stress functions in equations (3-6) were empirically developed by fitting the data located on the upper envelops, where it is assumed that transpiration is at a maximum rate (Macfarlane et al., 2004; Whitley et al., 2013). This partly explains why simulations best fitted sap flow measurements in spring using either the PM, MJS or BTA models.

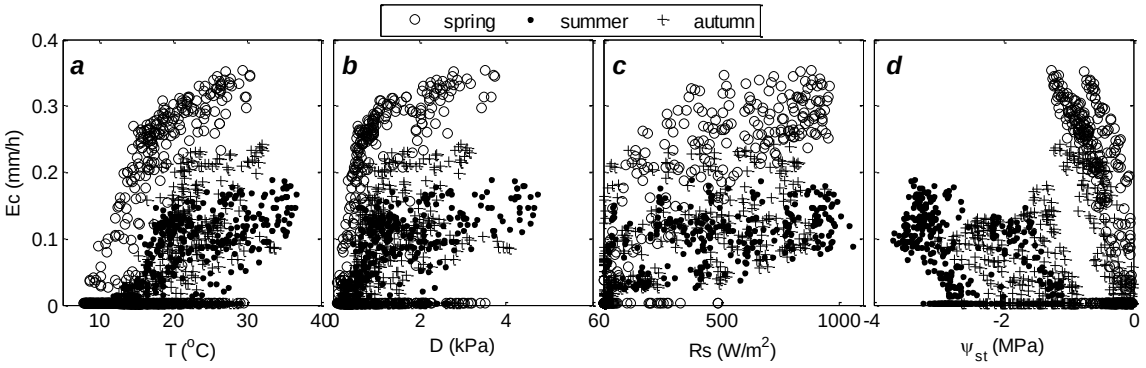

Figure 9 Relationship between tree water use and four environmental variables at the hourly scale using the same data in Figure 1

Figure 5-8 suggest that all PM, MJS and BTA models gave reasonable estimates of hourly tree water use in the three seasons, with regression slopes close to 1 and R^2 greater than 0.65. The MJS and BTA models are better than the PM indicated by higher R^2 and lower *RMSE*. In fact, the PM method contains more parameters and approximations throughout the simulations. First, g_c was calculated from sap flow data using the inversed Penman-Monteith equation; second, parameters in equations (2-6) and (10) were optimized using the calibration dataset, after which g_c was simulated with the validation dataset, and last, E_c was calculated using the Penman-Monteith equation and the simulated g_c. More approximations (e.g., aerodynamic resistance, net radiation over canopy, etc.) involved in the whole process resulted in the relatively poor degree of matching between simulations and observations. In contrast, models that calculate E_c directly from environmental variables have fewer parameters and avoid these approximations, leading to better simulations than the PM models.

3.2.3. Implications for water balance studies

In order to evaluate the applicability of the models for estimations of site water balance,

we summed the hourly transpiration from Figure 2*a*-*d*, and from Figure 5 and Figure 7 to daily values, and then compared the total E_c amounts to sap flow measurements in these 60 days (107.5 mm). Results are given in Figure 10. Most models slightly underestimated total E_c, except that PMJST overestimated E_c by 4.0% (sum of three seasons from Figure 5), PMB by 8.8% and 6.4% (summed from Figure 2*a*-*b* and Figure 5 respectively). Therefore, most models are considered acceptable for transpiration quantification in short-term (e.g. seasonal) water balance study; exceptions are PMJS4, PMJSψ and PMB in Figure 2*a*-*b*, with 9.7% and 26.4% underestimation, and 8.8% overestimation, respectively. Interestingly, the total E_c given by PM models in Figure 2*a*-*b* are considerably different from the totals in Figure 5 simulated separately in three seasons, which indicates that the parameters in the PM models are highly dependent on the data used to obtain the parameter values. On the contrary, the MJS and BTA models are more reliable regardless of using 60-day or 20-day data for parameters calibration.

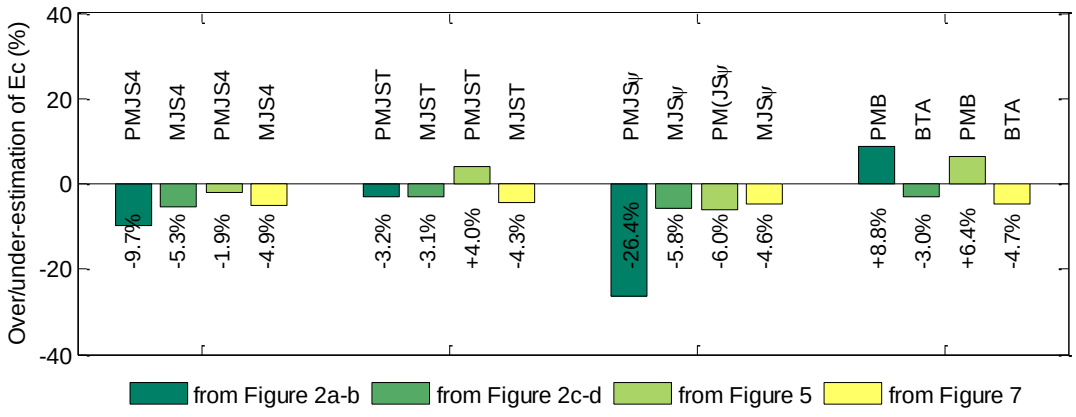

Figure 10 Comparison between total E_c summed from each hourly simulation and sap flow measurements. The numbers below the bars are the over/underestimated percentage by the

relevant models.

3.2.4. Daily E_c modeling

Simulated daily transpiration from the PM, MJS and BTA models in comparison to sap flow measurements is given in Figure 11 and Table 3. Models that contained four environmental variables gave the best daily E_c simulations. Models that contained a $f(\psi)$ generated better simulations than those without a $f(\psi)$. Soil water stress function had a stronger influence on transpiration modeling at the daily scale than the hourly scale, implied by comparing fitting results in Figure 3, Figure 6, Figure 8 and Figure 11. This is probably because stem water potential showed larger changes at a daily scale than an hourly scale. The PMJST, PMB and MJST and BTA models were not able to capture the daily dynamic of transpiration. It should be noted that the k and R^2 were obtained through linear regression with a zero intercept.

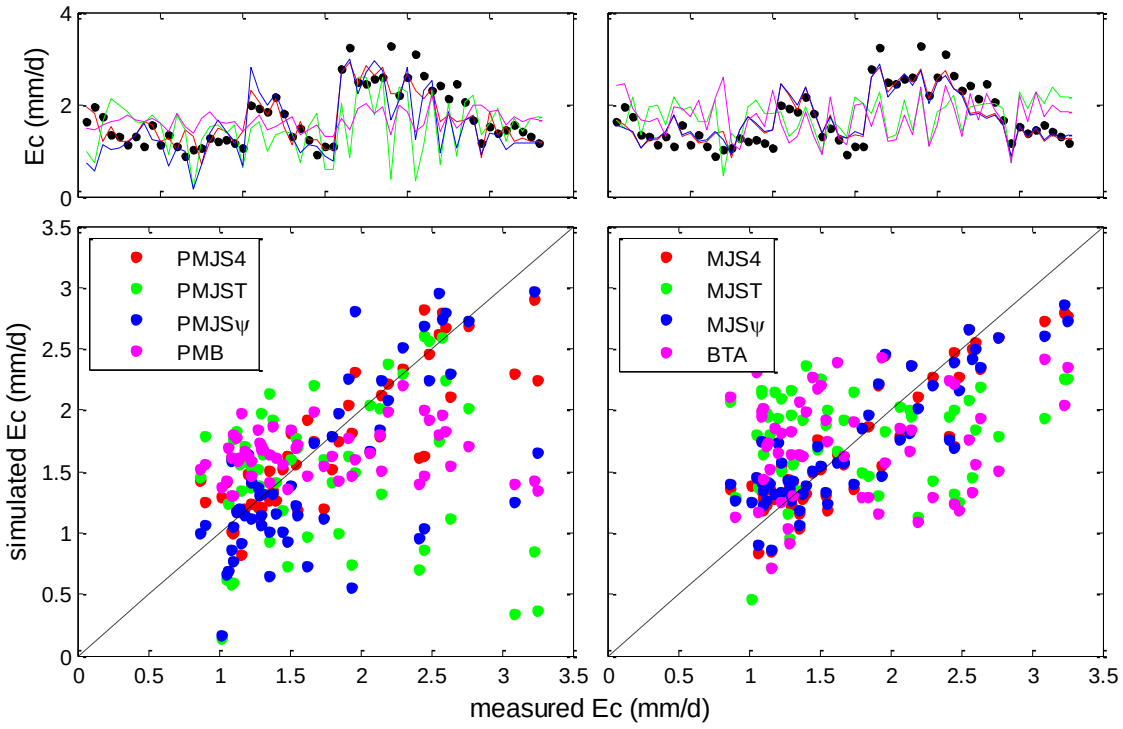

463

464 Figure 11 Comparison between simulated and measured transpiration at the daily scale.

465 Colored lines in the top plots correspond to the models indicated by the legends in the

466 bottom plots.

467 Table 3 Statistical results of comparison between simulated and measured daily transpiration by
468 the PM, MJS and BTA models in Figure 11. *k* is linear regression slope, R^2 is the coefficient of
469 determination, *RMSE* is root mean square error, in mm/d.

	PMJS4	**PMJST**	**PMJSψ**	**PMB**	**MJS4**	**MJST**	**MJSψ**	**BTA**
k	0.94	0.77	0.86	0.85	0.96	0.92	0.96	0.90
$\boldsymbol{R^2}$	0.73	0.00	0.47	0.01	0.78	0.02	0.77	0.01
RMSE	0.3309	0.8667	0.5686	0.6490	0.2966	0.6975	0.3054	0.7267

470

471 The fitting of daily sap flow measurements by PMJST and MJST degraded dramatically
472 compared to PMJS4 and MJS4, which implies that soil water function had a very strong
473 influence on daily E_c modeling. In addition, PMJS4 resulted in k=0.94, R^2=0.73 and

RMSE=0.3309 mm/d, better than those given by PMJSψ, while MJS4 gave similar simulations with MJSψ, indicating that the influence of *f(T)* on E_c modeling is more significant in the PM models than the MJS models. The poor performance of models BTA and PMB at a daily scale could be partly attributed to the parameter E_{max} in BTA E_c model, which limited the ability of BTA model to adjust its performance at the daily scale to reflect properly the effects of soil water availability on tree water uptake, but the limitation was not profound at the hourly scale, as the hour-to-hour maximum sap flow difference was smaller than the day-to-day difference.

3.3.Parameter values

The simulation of transpiration in current land surface models is often based on the Jarvis-Stewart scheme, so in this section we only compared the parameters in PMJS4, PMJST, PMJSψ, and also MJS4, MJST and MJSψ which are variants of the Jarvis-Stewart approach. By comparing the values of each parameter in different models across temporal scales (**Error! Reference source not found.**), we examine the universality of parameter values.

Some parameters have very small values compared to others, so for the convenience of comparison and display, we scaled the parameter values by multiplying different powers of ten. The results show that the maximum stomatal conductance g_{max} in the three PM models was similar at daily scale but varying at hourly scale in each season, generally larger in spring than in autumn and summer. The maximum transpiration rate E_{max} in the three MJS models was close at both daily scale and hourly scale, yet at hourly scale E_{max} was similar in the three models in spring, but varied much in summer and autumn. In different models, e.g., PMJS4, PMJST and PMJSψ, parameter k_{Rs} is similar at the same

time scales, i.e. daily or hourly scales in three seasons. Likewise, T_o, k_ψ and ψ_m are also similar among models at the same temporal scale. The parameter k_T in temperature function has big variations among models and across time scales, which renders the importance to input specific parameter values rather than a fixed value as adopted in some land surface models, e.g., 0.0016 in Chen and Dudhia (2001).

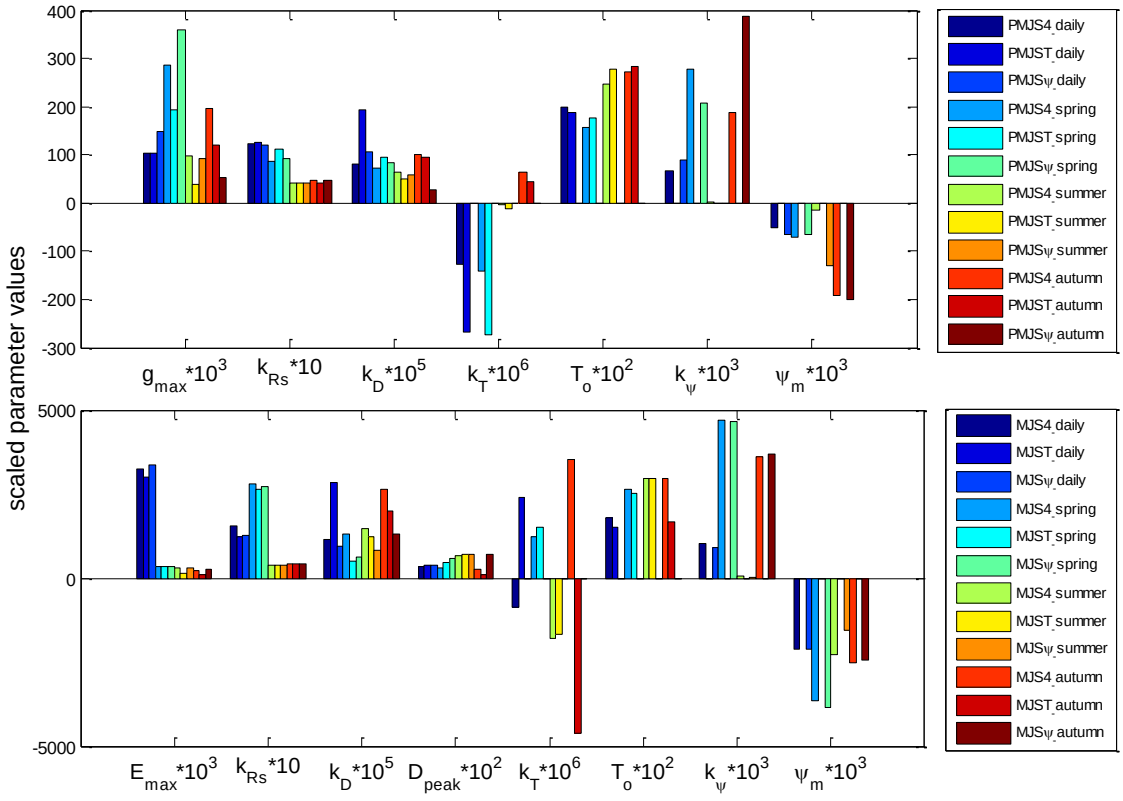

Figure 12 Parameter values multiplied by different powers of ten as shown in the figure for the convenience of comparison among models and across temporal scales.

The difference of daily and hourly parameter values in each model calls for attention in model applications at different temporal scales. Models need to be recalibrated when applied at a different temporal scale from which they were tuned initially. To demonstrate

this scale issue of parameters more clearly, we simulated hourly E_c with daily parameter values, and daily E_c with hourly parameter values using the PM models. No MJS models were tested because of the obvious difference of daily and hourly E_{max}, which will lead to a big difference in simulated hourly E_c using daily parameter values, and *vice versa*. The results demonstrate that using daily parameter values for hourly simulation and the other way around failed to reproduce the daily sap flow measurements, showing underestimation and overestimation, respectively (Figure 13). For instance, hourly simulation by PMJS4 model with daily parameter values underestimated daily E_c by about 45%, while daily simulation with hourly parameter values overestimated daily E_c by about 52% based on the same model.

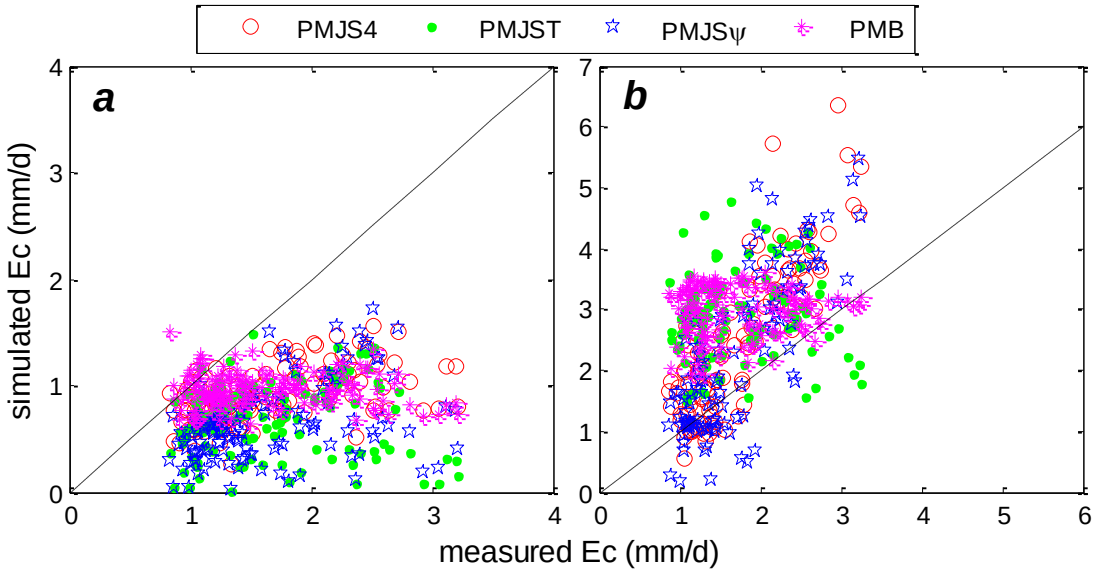

Figure 13 Comparison of simulated and measured E_c: (*a*) hourly simulation based on parameters calibrated with daily data; (*b*) daily simulation based on parameter values calibrated with hourly data

4. Conclusions

We compared three types of transpiration models, i.e. Penman-Monteith (PM) equation with g_c simulated from environmental variables by Jarvis-Stewart (JS) approach, modified JS approach (MJS) that links transpiration directly to environmental variables, and a simplified process-based model (BTA). The MJS models gave generally better simulations than the PM models at both daily and hourly scales. Nevertheless, at the daily scale, the best PM model performs comparable to the best MJS model. The BTA model used in this study is a simplified form of a process-based model, with the least number of parameters and sound physical interpretations of plant physiology, and is worth being promoted in future applications. However, BTA failed on the tree under water stress at the daily scale due to its treatment of soil water availability and other factors as an integrated parameter. The major advantage of the MJS and BTA models is the simplicity in terms of inputs and number of parameters.

Soil water availability function is important for E_c simulation at both temporal scales, particularly at the daily scale. For hourly E_c modeling the soil water function can be omitted in spring time in this study when there was sufficient water in the root-zone soil for vegetation water uptake. The influence of an air temperature function on model performance varies. Parameter values showed divergence across models and temporal scales, calling for attention to model application across temporal scales. At the hourly scale, parameters are better to be calibrated for each season rather than calibrated for all seasons for the improvement of long-term total tree water use modeling.

The results and conclusions are based on data observed from an individual tree. Another

three trees of the same species were observed to behave similarly in terms of water use in response to environmental conditions. We are aware that it may be difficult to extrapolate spatially to a large ecosystem composed of different species for transpiration estimation; however, the findings can still provide us some insights about the imperfection of the current transpiration model in terms of structure and parameterization schemes, e.g., careful selection of stress functions and parameter calibration strategy, thus aid for further model improvement and application for water balance studies.

Acknowledgements

This study is part of the first author's PhD projects in 2010-2014, co-funded by the *National Centre for Groundwater Research and Training* in Australia and the *China Scholarship Council*. We give thanks to Zijuan Deng and Xiang Xu for their assistance in the field. Constructive comments and suggestion from the anonymous reviewers are appreciated for significant improvement of the manuscript.

References

Alves, I. and Pereira, L.S., 2000. Modelling surface resistance from climatic variables? Agricultural Water Management, 42(3): 371-385.

Ball, J.H., L. E. Woodrow and Beny, J.A., 1987. A model predicting stomatal conductance and its contribution to the control of photosynthesis under different environmental conditions. In: J. Biggins (Editor), Progress in Photosynthesis research. Martinus Nijhoff, Providence, Rhode Island, USA, pp. 221-224.

Buckley, T.N. and Mott, K.A., 2002. Dynamics of stomatal water relations during the humidity response: implications of two hypothetical mechanisms. Plant Cell and Environment, 25(3): 407-419.

Buckley, T.N., Mott, K.A. and Farquhar, G.D., 2003. A hydromechanical and biochemical model of stomatal conductance. Plant Cell and Environment, 26(10): 1767-1785.

Buckley, T.N., Turnbull, T.L. and Adams, M.A., 2012. Simple models for stomatal conductance derived from a process model: cross-validation against sap flux data. Plant Cell and Environment, 35(9): 1647-1662.

Bunce, J.A., 2000. Responses of stomatal conductance to light, humidity and temperature

in winter wheat and barley grown at three concentrations of carbon dioxide in the field. Glob. Change Biol., 6(4): 371-382.
Chen, F. and Dudhia, J., 2001. Coupling an advanced land surface-hydrology model with the Penn State-NCAR MM5 modeling system. Part I: Model implementation and sensitivity. Monthly Weather Review, 129(4): 569-585.
Chen, F. et al., 1996. Modeling of land surface evaporation by four schemes and comparison with FIFE observations. Journal of Geophysical Research-Atmospheres, 101(D3): 7251-7268.
Choné, X. et al., 2001. Stem Water Potential is a Sensitive Indicator of Grapevine Water Status. Annals of Botany, 87(4): 477-483.
Dai, Y.J., Dickinson, R.E. and Wang, Y.P., 2004. A two-big-leaf model for canopy temperature, photosynthesis, and stomatal conductance. Journal of Climate, 17(12): 2281-2299.
Damour, G., Simonneau, T., Cochard, H. and Urban, L., 2010. An overview of models of stomatal conductance at the leaf level. Plant Cell and Environment, 33(9): 1419-1438.
Dewar, R.C., 2002. The Ball-Berry-Leuning and Tardieu-Davies stomatal models: synthesis and extension within a spatially aggregated picture of guard cell function. Plant Cell and Environment, 25(11): 1383-1398.
Dickinson, R.E., 1987. Evapotranspiration in global climate models. Adv Space Res, 7(11): 17-26.
Dickinson, R.E., Henderson-Sellers, A., Rosenzweig, C. and Sellers, P.J., 1991. Evapotranspiration Models with Canopy Resistance for Use in Climate Models - a Review. Agricultural and Forest Meteorology, 54(2-4): 373-388.
Dixon, M.A. and Tyree, M.T., 1984. A new stem hygrometer, corrected for temperature-gradients and calibrated against the pressure bomb. Plant Cell and Environment, 7(9): 693-697.
Dolman, A.J., Miralles, D.G. and de Jeu, R.A.M., 2014. Fifty years since Monteith's 1965 seminal paper: the emergence of global ecohydrology. Ecohydrology, 7(3): 897-902.
Eamus, D. and Froend, R., 2006. Groundwater-dependent ecosystems: the where, what and why of GDEs. Aust. J. Bot., 54(2): 91-96.
Findell, K.L. and Eltahir, E.A.B., 1997. An analysis of the soil moisture-rainfall feedback, based on direct observations from Illinois. Water Resour Res, 33(4): 725-735.
Ford, C.R., Hubbard, R.M., Kloeppel, B.D. and Vose, J.M., 2007. A comparison of sap flux-based evapotranspiration estimates with catchment-scale water balance. Agricultural and Forest Meteorology, 145(3-4): 176-185.
Franks, P.J., Cowan, I.R. and Farquhar, G.D., 1998. A study of stomatal mechanics using the cell pressure probe. Plant Cell and Environment, 21(1): 94-100.
Gao, Q., Zhao, P., Zeng, X., Cai, X. and Shen, W., 2002. A model of stomatal conductance to quantify the relationship between leaf transpiration, microclimate and soil water stress. Plant Cell and Environment, 25(11): 1373-1381.
Garcia, M. et al., 2013. Actual evapotranspiration in drylands derived from in-situ and satellite data: Assessing biophysical constraints. Remote Sensing of Environment, 131: 103-118.

622 Green, S., Clothier, B. and Jardine, B., 2003. Theory and practical application of heat
623 pulse to measure sap flow. Agron J, 95(6): 1371-1379.
624 Green, S. and Clothier, B.E., 1988. Water-use of kiwifruit vines and apple-trees by the
625 heat-pulse technique. J. Exp. Bot., 39(198): 115-123.
626 Gregory, P.J. and Nortcliff, S., 2013. Index, Soil Conditions and Plant Growth. Blackwell
627 Publishing Ltd, pp. 449-461.
628 Guan, H.D., Zhang, X.P., Skrzypek, G., Sun, Z. and Xu, X., 2013. Deuterium excess
629 variations of rainfall events in a coastal area of South Australia and its
630 relationship with synoptic weather systems and atmospheric moisture sources.
631 Journal of Geophysical Research-Atmospheres, 118(2): 1123-1138.
632 Hatton, T.J., Moore, S.J. and Reece, P.H., 1995. Estimating stand transpiration in a
633 Eucalyptus populnea woodland with the heat pulse method: measurement errors
634 and sampling strategies. Tree Physiology, 15(4): 219-27.
635 Ivanov, V.Y., Bras, R.L. and Vivoni, E.R., 2008. Vegetation-hydrology dynamics in
636 complex terrain of semiarid areas: 1. A mechanistic approach to modeling
637 dynamic feedbacks. Water Resour Res, 44. (3).
638 Jarvis, P.G., 1976. The interpretation of the variations in leaf water potential and stomatal
639 conductance found in canopies in the field. Philosophical Transactions of the
640 Royal Society of London. B, Biological Sciences, 273(927): 593-610.
641 Jasechko, S. et al., 2013. Terrestrial water fluxes dominated by transpiration. Nature,
642 496(7445): 347-+.
643 LeMone, M.A. et al., 2007. Influence of land cover and soil moisture on the horizontal
644 distribution of sensible and latent heat fluxes in southeast Kansas during
645 IHOP_2002 and CASES-97. Journal of Hydrometeorology, 8(1): 68-87.
646 Leuning, R., 1995. A Critical-Appraisal of A Combined Stomatal-photosynthesis Model
647 for C-3 Plants. Plant Cell and Environment, 18(4): 339-355.
648 Lhomme, J.P., Elguero, E., Chehbouni, A. and Boulet, G., 1998. Stomatal control of
649 transpiration: Examination of Monteith's formulation of canopy resistance. Water
650 Resour Res, 34(9): 2301-2308.
651 Macfarlane, C., White, D.A. and Adams, M.A., 2004. The apparent feed-forward
652 response to vapour pressure deficit of stomata in droughted, field-grown
653 Eucalyptus globulus Labill. Plant Cell and Environment, 27(10): 1268-1280.
654 Marshall, T.J., Holmes, J.W. and Rose, C.W., 1996. Soil physics. Cambridge University
655 Press, New York, USA, 21-28 pp.
656 Mascart, P., Taconet, O., Pinty, J.P. and Mehrez, M.B., 1991. Canopy Resistance
657 Formulation and Its Effect in Mesoscale Models - a Hapex Perspective.
658 Agricultural and Forest Meteorology, 54(2-4): 319-351.
659 Miralles, D.G., De Jeu, R.A.M., Gash, J.H., Holmes, T.R.H. and Dolman, A.J., 2011.
660 Magnitude and variability of land evaporation and its components at the global
661 scale. Hydrol Earth Syst Sc, 15(3): 967-981.
662 Mullins, C.E., 2001. Matric potential. In: C.E. Mullins and K.A. Smith (Editors), Soil and
663 Environmental Analysis: Physical Methods. Marcel Dekker, Inc., New York, pp.
664 65-93.
665 Noilhan, J. and Planton, S., 1989. A simple parameterization of land surface processes for
666 meteorological models. Monthly Weather Review, 117(3): 536-549.
667 Nortes, P.A., Pérez-Pastor, A., Egea, G., Conejero, W. and Domingo, R., 2005.

Comparison of changes in stem diameter and water potential values for detecting water stress in young almond trees. Agricultural Water Management, 77(1–3): 296-307.

O'Grady, A.P., Eamus, D., Cook, P.G. and Lamontagne, S., 2006. Comparative water use by the riparian trees Melaleuca argentea and Corymbia bella in the wet-dry tropics of northern Australia. Tree Physiology, 26(2): 219-228.

Palmer, A.R. et al., 2010. Towards a spatial understanding of water use of several land-cover classes: an examination of relationships amongst pre-dawn leaf water potential, vegetation water use, aridity and MODIS LAI. Ecohydrology, 3(1): 1-10.

Richter, H., 1997. Water relations of plants in the field: Some comments on the measurement of selected parameters. J. Exp. Bot., 48(306): 1-7.

Schlaepfer, D.R. et al., 2014. Terrestrial water fluxes dominated by transpiration: Comment. Ecosphere, 5(5): 1-9.

Schlesinger, W.H. and Jasechko, S., 2014. Transpiration in the global water cycle. Agricultural and Forest Meteorology, 189-190: 115-117.

Schulze, E.D. et al., 1996. Rooting depth, water availability, and vegetation cover along an aridity gradient in Patagonia. Oecologia, 108(3): 503-511.

Sommer, R. et al., 2002. Transpiration and canopy conductance of secondary vegetation in the eastern Amazon. Agricultural and Forest Meteorology, 112(2): 103-121.

Stewart, J.B., 1988. Modeling surface conductance of pine forest. Agricultural and Forest Meteorology, 43(1): 19-35.

Tuzet, A., Perrier, A. and Leuning, R., 2003. A coupled model of stomatal conductance, photosynthesis and transpiration. Plant Cell and Environment, 26(7): 1097-1116.

Vandegehuchte, M.W. et al., 2014. Long-term versus daily stem diameter variation in co-occurring mangrove species: Environmental versus ecophysiological drivers. Agricultural and Forest Meteorology, 192–193(0): 51-58.

Verhoef, A. and Egea, G., 2014. Modeling plant transpiration under limited soil water: Comparison of different plant and soil hydraulic parameterizations and preliminary implications for their use in land surface models. Agricultural and Forest Meteorology, 191: 22-32.

Vrugt, J.A. et al., 2009. Accelerating Markov Chain Monte Carlo Simulation by Differential Evolution with Self-Adaptive Randomized Subspace Sampling. Int. J. Nonlinear Sci. Numer. Simul., 10(3): 273-290.

Wang, H., Guan, H., Deng, Z. and Simmons, C.T., 2014. Optimization of canopy conductance models from concurrent measurements of sap flow and stem water potential on Drooping Sheoak in South Australia. Water Resour Res, 50(7): 6154-6167.

Wang, L. et al., 2010. Partitioning evapotranspiration across gradients of woody plant cover: Assessment of a stable isotope technique. Geophys Res Lett, 37.

Whitley, R., Medlyn, B., Zeppel, M., Macinnis-Ng, C. and Eamus, D., 2009. Comparing the Penman-Monteith equation and a modified Jarvis-Stewart model with an artificial neural network to estimate stand-scale transpiration and canopy conductance. Journal of Hydrology, 373(1-2): 256-266.

Whitley, R. et al., 2013. Developing an empirical model of canopy water flux describing the common response of transpiration to solar radiation and VPD across five

contrasting woodlands and forests. Hydrological Processes, 27(8): 1133-1146.
Wright, I.R., Manzi, A.O. and Darocha, H.R., 1995. Surface conductance of amazonian pasture - model application and calibration for canopy climate. Agricultural and Forest Meteorology, 75(1-3): 51-70.
Yang, Y. et al., 2013. Examination and parameterization of the root water uptake model from stem water potential and sap flow measurements. Hydrological Processes, 27(20): 2857-2863.